Integrated Genome-Wide DNA Copy Number and Expression Analysis Identifies Distinct Mechanisms of Primary Chemoresistance in Ovarian Carcinomas

Dariush Etemadmoghadam,[1,2] Anna deFazio,[3] Rameen Beroukhim,[4] Craig Mermel,[4] Joshy George,[1,2] Gad Getz,[4] Richard Tothill,[1] Aikou Okamoto,[6] Maria B. Raeder,[7] AOCS Study Group,[1,3,10] Paul Harnett,[3] Stephen Lade,[1] Lars A. Akslen,[8] Anna V. Tinker,[1] Bianca Locandro,[1] Kathryn Alsop,[1] Yoke-Eng Chiew,[3] Nadia Traficante,[1] Sian Fereday,[1] Daryl Johnson,[1] Stephen Fox,[1] William Sellers,[5] Mitsuyoshi Urashima,[6] Helga B. Salvesen,[7,9] Matthew Meyerson,[4] and David Bowtell[1,2]

Abstract

Purpose: A significant number of women with serous ovarian cancer are intrinsically refractory to platinum-based treatment. We analyzed somatic DNA copy number variation and gene expression data to identify key mechanisms associated with primary resistance in advanced-stage serous cancers.

Experimental Design: Genome-wide copy number variation was measured in 118 ovarian tumors using high-resolution oligonucleotide microarrays. A well-defined subset of 85 advanced-stage serous tumors was then used to relate copy number variation to primary resistance to treatment. The discovery-based approach was complemented by quantitative-PCR copy number analysis of 12 candidate genes as independent validation of previously reported associations with clinical outcome. Likely copy number variation targets and tumor molecular subtypes were further characterized by gene expression profiling.

Results: Amplification of 19q12, containing cyclin E (*CCNE1*), and 20q11.22-q13.12, mapping immediately adjacent to the steroid receptor coactivator *NCOA3*, was significantly associated with poor response to primary treatment. Other genes previously associated with copy number variation and clinical outcome in ovarian cancer were not associated with primary treatment resistance. Chemoresistant tumors with high *CCNE1* copy number and protein expression were associated with increased cellular proliferation but so too was a subset of treatment-responsive patients, suggesting a cell-cycle independent role for *CCNE1* in modulating chemoresponse. Patients with a poor clinical outcome without *CCNE1* amplification overexpressed genes involved in extracellular matrix deposition.

Conclusions: We have identified two distinct mechanisms of primary treatment failure in serous ovarian cancer, involving *CCNE1* amplification and enhanced extracellular matrix deposition. *CCNE1* copy number is validated as a dominant marker of patient outcome in ovarian cancer.

Standard of care for women with advanced-stage ovarian cancer involves primary cytoreductive surgery followed by adjuvant chemotherapy with a platinum-based agent, often regarded as the most active component, and a taxane (1). Although response rates to first-line treatment are high, 20% to 25% of cases relapse during or soon after the cessation of primary therapy (2). The ability to predict treatment response and the development of therapies to counter primary chemoresistance are key goals of ovarian cancer research. Known platinum-resistance mechanisms include reduced drug delivery

Authors' Affiliations: [1]Peter MacCallum Cancer Centre, Melbourne, Victoria, Australia; [2]Department of Biochemistry and Molecular Biology, University of Melbourne, Parkville, Victoria, Australia; [3]Westmead Institute for Cancer Research, University of Sydney at Westmead Millennium Institute, Westmead Hospital, New South Wales, Australia; [4]Broad Institute of Massachusetts Institute of Technology and Harvard, and [5]Novartis Institutes for Biomedical Research, Cambridge, Massachusetts; [6]Jikei University School of Medicine, Tokyo, Japan; [7]Department of Obstetrics and Gynecology, Haukeland University Hospital, and [8]The Gade Institute and [9]Institute of Clinical Medicine, The University of Bergen, Bergen, Norway; and [10]Queensland Institute of Medical Research, Brisbane, Queensland, Australia

Received 6/18/08; revised 8/17/08; accepted 8/18/08; published OnlineFirst 02/03/2009.

Grant support: U.S. Army Medical Research and Materiel Command under DAMD17-01-1-0729, The Cancer Council Victoria, Queensland Cancer Fund, The Cancer Council New South Wales, The Cancer Council South Australia, The Cancer Foundation of Western Australia, The Cancer Council Tasmania and the National Health and Medical Research Council of Australia (NHMRC), the U.S. Department of Defense grant PC040638 and the Dana-Farber/Harvard Cancer Center Prostate SPORE.

The costs of publication of this article were defrayed in part by the payment of page charges. This article must therefore be hereby marked *advertisement* in accordance with 18 U.S.C. Section 1734 solely to indicate this fact.

Note: Supplementary data for this article are available at Clinical Cancer Research Online (http://clincancerres.aacrjournals.org/).

Requests for reprints: David Bowtell, Peter MacCallum Cancer Centre. Locked Bag 1, A'Beckett Street, Melbourne, VIC 8006, Australia. Phone: 613-96561356; Fax: 613-96561414; E-mail: d.bowtell@petermac.org.

doi:10.1158/1078-0432.CCR-08-1564

Translational Relevance

Resistance to chemotherapy in women with advanced-stage ovarian cancer is a major clinical problem. We describe two distinct molecular mechanisms of resistance that have future clinical relevance for response prediction and the development of novel therapeutic strategies. The key finding that *CCNE1* (cyclin E) amplification is strongly associated with treatment-resistance in ovarian carcinomas is consistent with previous associations with poor survival reported for ovarian and other cancer types. Amplification status of *CCNE1* therefore has potential for therapeutic exploitation, whereby patients carrying *CCNE1* amplification may benefit from novel, cyclin-related targeted treatments. A second group of patients, exhibiting an alternative mode of resistance associated with host tissue elements and reactive stroma, is likely to benefit from therapeutic strategies that target different activation pathways.

to target DNA and failure of cells to initiate cell death in response to platinum-induced DNA damage, due to defects in DNA damage recognition, repair, and apoptosis (3). However, most mechanistic studies on platinum resistance have been done using *in vitro* cell models and few have been shown to be relevant in the clinical setting (3).

Chromosomal aberrations reflect oncogene activation and loss of tumor suppressor genes (4), and global surveys of DNA gain or loss have been considered a fertile area to search for determinants of chemoresistance and survival in ovarian cancer. Comparative genomic hybridization on metaphase spreads (5, 6) has been superseded by higher-resolution array comparative genomic hybridization using large mapped insert clones (7, 8) or oligonucleotide probes (9). Although a number of chromosomal regions (6–8, 10, 11) and individual genes, including *FGF1* (9), *EVI1* (12), *CCNE1* (13, 14), *PRKCI* (15), *RSF1* (16), *RAB25* (17), *BRCA1* (18), *ERBB2* (19, 20), *MUC1* (21), *IGF2R* (22), *ZNF217* (23), and *MYC* (24), have reported copy number variation linked to patient outcome in ovarian cancer, most have not yet been validated in independent studies until now.

We did both a discovery and a validation study in a clinically well-characterized sample population of ovarian tumors, comprising the largest cohort to be analyzed by both copy number and gene expression microarrays to date. High-resolution oligonucleotide copy number analysis on 118 high-grade serous ovarian cancers, including 85 tumors representing a carefully selected patient cohort, were used to identify recurrent regions of genomic change associated with primary treatment response. In parallel, we did the first direct comparison of 12 genes previously associated with copy number variation and clinical outcome in ovarian cancer, using quantitative-PCR (qPCR).

Among six regions of copy number variation that were differentially altered in patients with either a good or poor response to primary treatment, we show that amplification of 19q12, associated with *CCNE1*, and 20q13, mapped immediately adjacent to *NCOA3*, was significantly associated with chemoresistance.

Importantly, *CCNE1* was the only previously reported copy number variation associated with poor outcome in ovarian cancer validated as a marker for primary chemoresistance. We also identify a group of chemoresistant cases without *CCNE1* amplification or increased cellular proliferation, which are characterized by increased expression of extracellular matrix–related genes. These data imply that patients without *CCNE1* amplification and a poor response to treatment follow a distinct molecular pathway to those cases with *CCNE1* amplification, possibly involving extracellular matrix deposition from activated stroma.

Materials and Methods

Patients. The study population consisted of 118 patients diagnosed with epithelial ovarian, primary peritoneal, or fallopian tube cancer from 1988 to 2005 (Supplementary Table S1). Primary treatment failure occurs in a minority of patients and is influenced by the adequacy of surgical debulking. We therefore preselected a cohort of patients from four studies to obtain adequate numbers of responsive and resistant patients in our cohort: the Australian Ovarian Cancer Study (25), Westmead Hospital (Sydney, Australia), Haukeland University Hospital of Bergen (Bergen, Norway), and Jikei University (Tokyo, Japan). This project had institutional ethics review board approval at all participating centers.

Clinical treatment and definitions. Patients underwent laparotomy for diagnosis, staging, and tumor debulking, and subsequently received first-line platinum-based chemotherapy. Tumor material for the study was excised at the time of primary surgery, prior to the administration of chemotherapy. Surgical staging was assessed in accordance with Fédération Internationale des Gynaecologistes et Obstetristes (FIGO) classification. Optimal debulking was defined as ≤1 cm (diameter) residual disease, and suboptimal debulking was >1 cm (diameter) residual disease.

A subset of 85 cases selected from the total cohort of 118 tumors was used to investigate response to therapy and survival (Table 1). The "clinical cohort" included cases that had stage III or IV serous invasive disease and received treatment including a platinum-based agent, carboplatin or cisplatin, administered without delay (within 6 wk of surgery) and completed adequately (≥4 cycles of platinum) unless disease progression was evident while on first-line treatment. Patients who had received neoadjuvant chemotherapy were excluded.

The cohort was further stratified into platinum-"resistant" and treatment-"responsive" patients based on progression-free interval. Less than 6 mo to disease progression was chosen as an end point to define resistant cases due to its clinical relevance in identifying platinum-resistant disease (1). Resistant cases either progressed on primary treatment, had stable disease (evidenced by persistently elevated CA125), or had a partial or complete CA125 response and relapsed within 6 mo from the end of primary chemotherapy.

Given that suboptimal debulking can contribute to rapid disease progression (26), any case with >2 cm residual disease or unknown debulking status was excluded from the resistant group. Treatment-responsive patients had a complete pathologic response and/or no evidence of disease progression for a minimum of 9 mo from the end of primary treatment.

Progressive disease was determined based on CA125 marker and imaging according to Response Evaluation Criteria in Solid Tumors guidelines modified for ovarian cancer (27, 28), or on clinical examination. Progression-free survival (PFS) was calculated as the interval between the end of primary treatment to disease progression; overall survival (OS) was defined as the time interval between the date of surgery and the date of death from any cause.

Histologic subtype and tumor grade (according to WHO criteria) were derived from the diagnostic pathology reports. Although central

Table 1. Clinical cohort patient clinicopathologic characteristics

	Responsive	Resistant	*P*
Age			
Mean, y (SD)	57 (10)	59 (13)	0.19*
Range, y	36-78	23-85	
Stage			
III	46 (88%)	29 (88%)	1.00 †
IV	6 (12%)	4 (12%)	
Grade			
Low (well differentiated)	4 (8%)	1 (3%)	0.43 †
Medium	22 (42%)	11 (33%)	
High (poorly differentiated)	24 (46%)	19 (58%)	
Unknown	2 (4%)	2 (6%)	
Residual disease			
≤1 cm	26 (50%)	20 (61%)	0.82 †
>1 cm	19 (37%)	13 (39%)	
Unknown	7 (13%)	0 (0%)	
Primary treatment			
Pt-based	2 (4%)	4 (12%)	0.08 †
Pt-based + taxane	40 (77%)	17 (52%)	
Pt-based + other	1 (2%)	2 (6%)	
Pt-based + taxane + other	9 (17%)	10 (30%)	
PFS (from end of primary T_x)			
Median mo	17.50	3.75	<0.001 ‡
(95% CI)	(14.6-26.9)	(2.57-4.87)	
Events	40 (77%)	33 (100%)	
OS (from surgery)			
Median y (95% CI)	5.07 (4.55-6.72)	1.63 (1.40-2.66)	<0.001 ‡
Events	22 (42%)	28 (85%)	
Total cases (n = 85)	52	33	

NOTE: Calculated *P* values from *Wilcoxon rank sum test, †Fisher test, or ‡Cox proportional hazard model.
Abbreviations: 95% CI, 95% confidence interval; Pt, platinum-based agent cisplatin or carboplatin.

pathology review of all cases was not done, H&E-stained sections flanking the fresh-frozen tissue used for nucleic acid extraction were reviewed by collaborating pathologists to assess cellular composition and confirm histology. Samples were only included if histology as assessed from the fresh-frozen slide review was consistent with the original pathology report.

Nucleic acid extraction. DNA was extracted from whole tumor tissue for samples with ≥80% neoplastic cells. For samples with <80% overall tumor cells, needle dissection of serial tumor sections was done to enrich for the epithelial fraction prior to DNA extraction. Needle-dissected samples were stained with cresyl-violet (Ambion) to facilitate morphologic distinction between tumor and stromal elements. Genomic DNA was extracted using a DNeasy kit (Qiagen) according to the manufacturer's protocol and quantified by spectrophotometry. Total RNA from whole tumor samples was isolated by phenol-chloroform extraction (Invitrogen) and purified using Qiagen RNeasy columns (Qiagen) according to the standard protocol. RNA quality was assessed using the Bioanalyzer 2100 (Agilent) prior to gene expression profiling.

Single nucleotide polymorphism mapping and expression microarrays. Affymetrix 50K *XbaI* single nucleotide polymorphism (SNP) mapping arrays were used for genome-wide copy number analysis (29). Affymetrix U133plus2.0 arrays were used to measure gene expression of 47,000 transcripts including 38,500 characterized genes. The mapping and expression array assays were done according to the manufacturer's protocol (Affymetrix). Further experimental details are given in Supplementary Methods.

SNP microarray data analysis. Copy number variation frequency and amplitude (gain, amplification, single copy loss, or homozygous deletion) was examined to determine the significance of copy number variation using the Genomic Identification of Significant Targets in Cancer (GISTIC) method as described previously (30). After microarray and copy number normalization steps were applied, a G score was generated for each SNP to assess copy number variation across all samples in the tumor set. A G score was calculated considering frequency of copy number change (f) and mean copy number amplitude (c) equal to $G_i^{amp} = f_i^{amp} \times c_i^{amp}$ for amplifications and $G_i^{del} = -f_i^{del} \times c_i^{del}$ for deletions. The background distribution of random G scores was estimated by permutation testing of all marker labels and each G score then assigned a false discovery rate–corrected significance (q value). A q value cutoff of 0.25 was used to define significant regions of recurrent copy number variation. Within each region, the locus with minimal q value was also identified as the primary target or peak copy number variation, while allowing for one randomly aberrant sample that may have shifted the peak boundary (29).

GISTIC analysis was then done on the treatment-responsive and treatment-resistant class tumors separately to identify copy number variations that were either unique to one group or varied in frequency or amplitude of copy number variation occurrence between classes. The difference in calculated G scores for each peak SNP (Gi) identified by GISTIC in either the treatment-responsive and/or treatment-resistant classes was calculated, where $\Delta G_i = G_i^{Resistant} - G_i^{Responsive}$. Each ΔG score was then assigned a false discovery rate–corrected ΔG significance (ΔG P value) by further permutation testing of all marker values to generate the expected chance or background distribution of ΔG scores. Peak copy number variation with ΔG P values < 0.05 were classified as differentially mapped peaks (DMP).

qPCR. SNP-based copy number was validated by qPCR on a subset of 52 cases for which DNA was available. PCR primers were designed using Primer3 (31) and selected to avoid known SNPs and not to amplify products with homology to other sequences (Supplementary Table S2). To evaluate consistency of results, two independent primer sets were used to amplify each gene of interest, except for *MYC* and for *MUC1/FGF1* on which previously published primer sequences were used (9, 21). Real-time qPCR was done using SYBR Green qPCR on the 7900HT Fast Real-Time PCR system (Applied Biosystems) as described in Supplementary Methods.

Expression microarray data analysis. Matched SNP and expression data were available for 52 samples. In addition, 37 samples that met our clinical criteria but were not assayed by SNP array had expression data available (25). The combined data set (n = 89; Supplementary Table S3) was used to identify gene probe-sets within copy number variation regions with a significant correlation with clinical outcome. Transcription profiling was also used to further characterize molecular subtypes of chemoresistant patients as detailed in Supplementary Methods.

Immunohistochemistry. Immunohistochemistry was done according to standard protocols using antibodies against CCNE1 (Clone 13A3; LabVision) and Ki-67 (Clone MIB1; Dako) on tissue microarrays containing a subset of stage III/IV, serous tumors from the clinical cohort as defined above (see Supplementary Methods). Staining was assessed by a pathologist and images captured using an Olympus BX51 microscope.

Results

Significant regions of amplification and deletion in ovarian tumors. High-resolution analysis of a large cohort of tumors provided an unprecedented view of common copy number variation in ovarian cancer. Data were analyzed using a statistically-robust algorithm (GISTIC) that sequentially filters

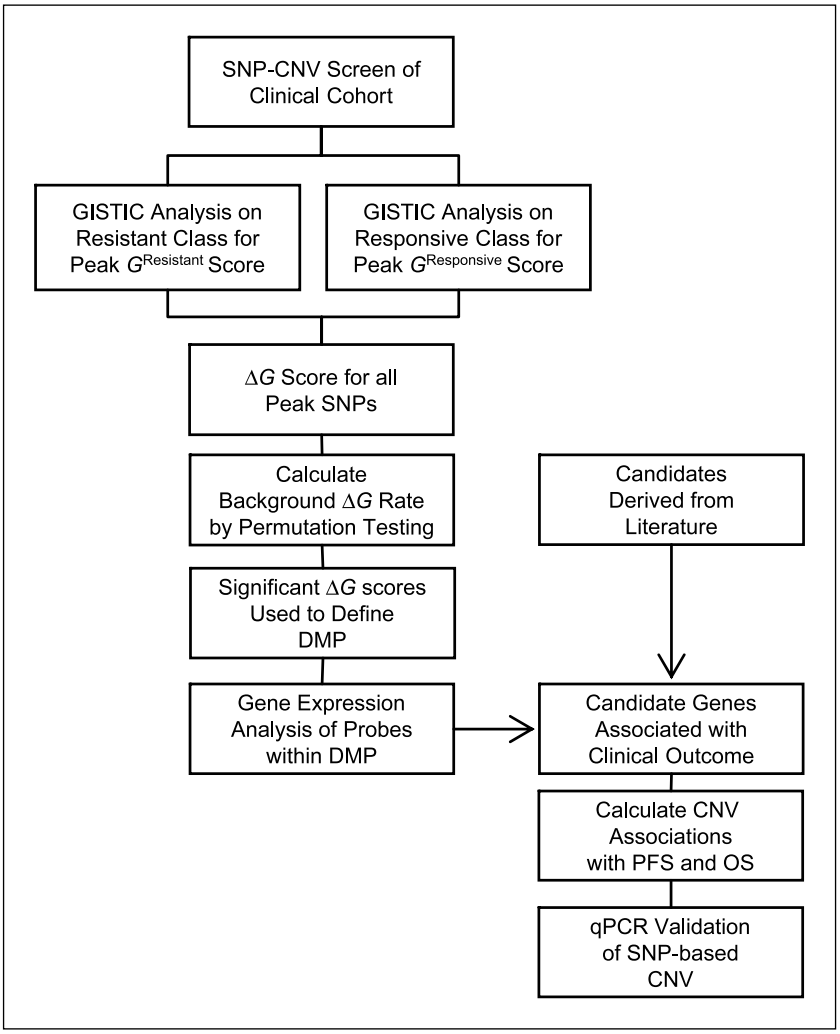

Fig. 1. Schematic of experimental design used to identify copy number variation changes associated with response to primary treatment.

the data and creates a probabilistic estimate of the most significant regions of copy number variation and minimal or peak loci within each region, likely to contain "driver" oncogenes or tumor suppressors. GISTIC analysis includes a quality control step in which tumor samples with insignificant detectable copy number variation are removed from the analysis (30). From an original cohort of 128, 10 samples were excluded from the final analysis due to suspected stromal contamination. Supplementary Fig. S1 shows summary information on copy number variation in the cohort of 118 cases, where regions of gain or loss are depicted according the significance of copy number variation accounting for copy number frequency and magnitude. Genome coordinates for each region of copy number variation in addition to the minimally targeted peak(s) are given in Supplementary Table S4. A total of 19 amplification peaks and 22 deletion peaks were identified. This study focused on regions of amplification associated with primary treatment failure; further analysis of potential driver genes in regions of amplification and deletion will be described elsewhere.

Table 2. Differentially mapped peaks from comparative copy number analysis of treatment resistant and responsive classes

CNV	Cytoband (peak)	Peak position (Mb)	Enriched in response class	ΔG score	*P*
Amplification	19q12	34.39-35.02	Resistant	0.20	0.003
Amplification	20q11.22-q13.12	33.52-44.89	Resistant	0.11	0.016
Amplification	5p15.31	8.28-11.14	Resistant	0.12	0.024
Amplification	6p25.1	6.31-8.47	Responsive	-0.09	0.037
Deletion	22q13.31	46.61-49.02	Responsive	-0.10	0.045
Deletion	2q34	209.49-209.52	Responsive	-0.18	0.046

NOTE: Peaks with FDR-corrected ΔG score $P < 0.05$ from 71 tested regions shown.

Amplification of 19q12 and 20q11.22-q13.12 is significantly associated with primary chemoresistance. We next identified regions of copy number variation associated with clinical course following primary treatment (Fig. 1). To ensure adequate numbers of cases to investigate primary treatment response, we carefully selected a cohort of primary invasive serous ovarian cancer patients of 33 poor-outcome (resistant) and 52 good-outcome (treatment-responsive) cases, obtained from Australian, Japanese, and Norwegian sample sets. The two groups were well balanced for prognostic features (patient age, FIGO stage, histopathologic grade, and extent of residual disease following debulking surgery), with no statistically significant difference between any tested variable except PFS and OS (Table 1).

Copy number analysis done separately on the resistant and treatment-responsive samples identified a total of 20 amplification peaks and 20 deletion peaks in the responsive tumors, and 14 amplification peaks and 17 deletion peaks in the resistant class (Supplementary Tables S5 and S6).

The frequency and amplitude (*G* score) of each peak copy number variation was then compared between classes to identify genomic regions that were differentially amplified or deleted between response classes. We chose to focus only on the identified peak copy number variation (total of 71 distinct or overlapping peaks between both classes) as these regions were considered most likely to contain copy number variation–targeted genes important in tumorigenesis and disease progression. By using only peak SNPs, as opposed to all >50,000 SNP makers, we also limit detection of chance correlations with outcome variables associated multiple-hypothesis testing.

Six class-specific differentially mapped peaks (DMP) were defined (Table 2). The two highest-ranking DMPs were amplification of 19q12 (incorporating *CCNE1*) and 20q11.22-q13.12 (immediately adjacent to *NCOA3*), which were more commonly associated with the resistant response class. Both 19q12 and 20q11.22-q13.12 copy numbers were also statistically significantly associated with survival (PFS and/or OS) in which time to clinical progression was considered as a continuous variable (Table 3).

Figure 2 shows the *G* score profile for chromosome 19 and chromosome 20 using all tumors and for each response class individually. The effect of class-specific tumor heterogeneity on *G* score values is evident for both DMP amplicons, where decreased *G* score values were observed in the combined analysis (Fig. 2A and C) compared with an analysis of specific patient subgroups (Fig. 2B and D).

To identify the most likely driver genes within the amplicons, gene expression values for all probes within the 19q12 and 20q11.22-q13.12 DMPs were correlated with PFS and OS. Genes that were significantly correlated ($P < 0.05$) with either PFS or OS are shown in Supplementary Table S7. These include *CCNE1*, contained within the 19q12 amplicon, and *NCOA3*, although not within the peak, maps immediately distal (~0.7 Mb) to the 20q11.22-q13.12 amplicon.

In addition to identifying copy number associations between copy number and treatment response in identified peak copy number variations, we also directly tested copy number associations with PFS and OS of 12 literature-derived candidates previously associated with clinical course in ovarian cancer but which may not have been localized within significant peak copy number variation as determined by GISTIC analysis (Table 3). Genes included amplification of *CCNE1*, also identified by our screen, in addition to *ERBB2*, *FGF1*, *MDS1/EVI1*, *MUC1*, *MYC*, *PRKCI*, *RAB25*, *RSF1*, *ZNF217*, and deletion of *BRCA1* and *IGF2R* (Table 3).

Gene copy number was estimated by SNP microarray using the copy number of SNPs within each gene or the two flanking SNP markers. Of the tested genes *CCNE1* was significantly associated with shorter OS, consistent with its localization within the 19q12 DMP associated with the treatment-resistant class, and *ZNF217* with shorter PFS and OS, despite not being associated with a primary treatment response group peak copy number variation specifically (Table 3).

Table 3. Survival analysis of candidate gene copy number detected by SNP-based screen and/or previously reported

Gene	Candidate selection	Frequency responsive	Frequency resistant	PFS (*P*)	OS (*P*)
Amplifications					
CCNE1	Identified in SNP-CNV screen*	9.6%	27.3%	0.264	0.019
ERBB2	Lassus et al., 2004 †	0.0%	3.0%	0.840	0.101
FGF1	Birrer et al., 2007	1.9%	6.1%	0.121	0.280
MDS1/EVI1	Nanjundan et al., 2007	44.2%	39.4%	0.431	0.808
MUC1	Takano et al., 2004	17.3%	6.1%	0.875	0.286
MYC	Baker et al., 1990	57.7%	51.5%	0.752	0.829
NCOA3	Identified in SNP-CNV screen	13.5%	27.3%	0.009	0.004
PRKCI	Eder et al., 2005	44.2%	45.5%	0.181	0.267
RAB25	Cheng et al., 2004	17.3%	6.1%	0.875	0.286
RSF1 (HBXAP)	Shih Ie et al., 2005	23.1%	15.2%	0.121	0.091
ZNF217	Peiro et al., 2002 ‡	21.2%	27.3%	0.022	0.008
Deletions					
BRCA1	Kato et al., 2004	38.5%	36.4%	0.814	0.110
IGF2R	Makhija et al., 2003	44.2%	21.2%	0.376	0.499

Abbreviation: CNV, copy number variation.
*Also see Mayr et al., 2006 and Farley et al., 2003.
† Also see Slamon et al., 1989.
‡ Also see Dimova et al., 2005.

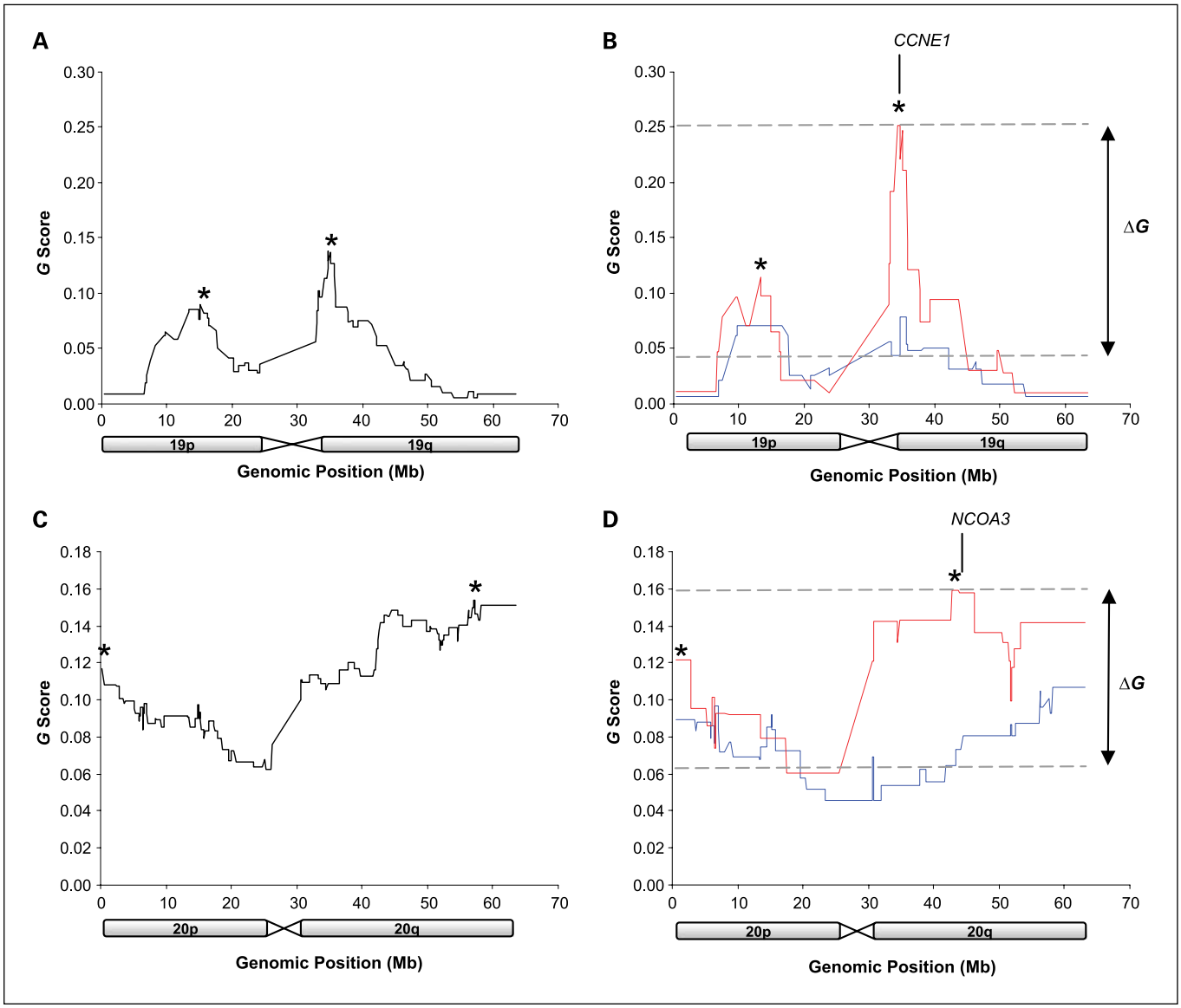

Fig. 2. GISTIC *G* score profile of chromosomes 19 (*A* and *B*) and 20 (*C* and *D*). *G* scores are shown for all ovarian samples (*A* and *C*) and for responsive (*blue*) and resistant (*red*) samples separately (*B* and *D*). *, mapped copy number variation peaks within regions of copy number variation. Regions with significant Δ*G* values used to define DMP are indicated.

Microarray-based copy number assessment of the two highest-ranking DMPs and the remaining literature-derived candidates were technically validated by qPCR (Table 3). A high degree of concordance between SNP and qPCR data was observed for most genes (median Pearson correlation coefficient of ~0.7), but *FGF1 MUC1*, *PRKC1*, and *RAB25* showed Pearson coefficients of <0.5 (Supplementary Fig. S2). The difference may relate to limitations of the microarray platform; although the 50K SNP arrays used in this study provided very high-resolution genome-wide analysis of copy number variation, coverage of all areas was not equal. For example, *RAB25* and *MUC1*, both previously reported to be associated with copy number variation and clinical outcome in ovarian cancer (17, 21), reside in regions with relatively poor SNP representation on the 50K SNP platform. Given these results, we also tested the association between qPCR-determined copy number of the four genes with clinical outcome to supplement data from the SNP-based analysis.

Copy number variation was shown for *FGF1*, *MUC1*, *PRKC1*, and *RAB25* by qPCR, but their association with clinical outcome remained insignificant (Supplementary Table S8). In comparison with the SNP microarrays, qPCR analysis detected a substantially larger number of cases with amplification of the *FGF1* and *RAB25* loci. In contrast to previous findings (9), however, we still did not find an association between *FGF1* amplification and outcome in our cohort. A trend towards amplification and resistance was evident for *RAB25*, but this did not reach statistical significance. It is possible that the smaller sample size used for the qPCR analysis, compared with the SNP experiments, may have adversely affected the ability to detect a significant association between copy number and outcome.

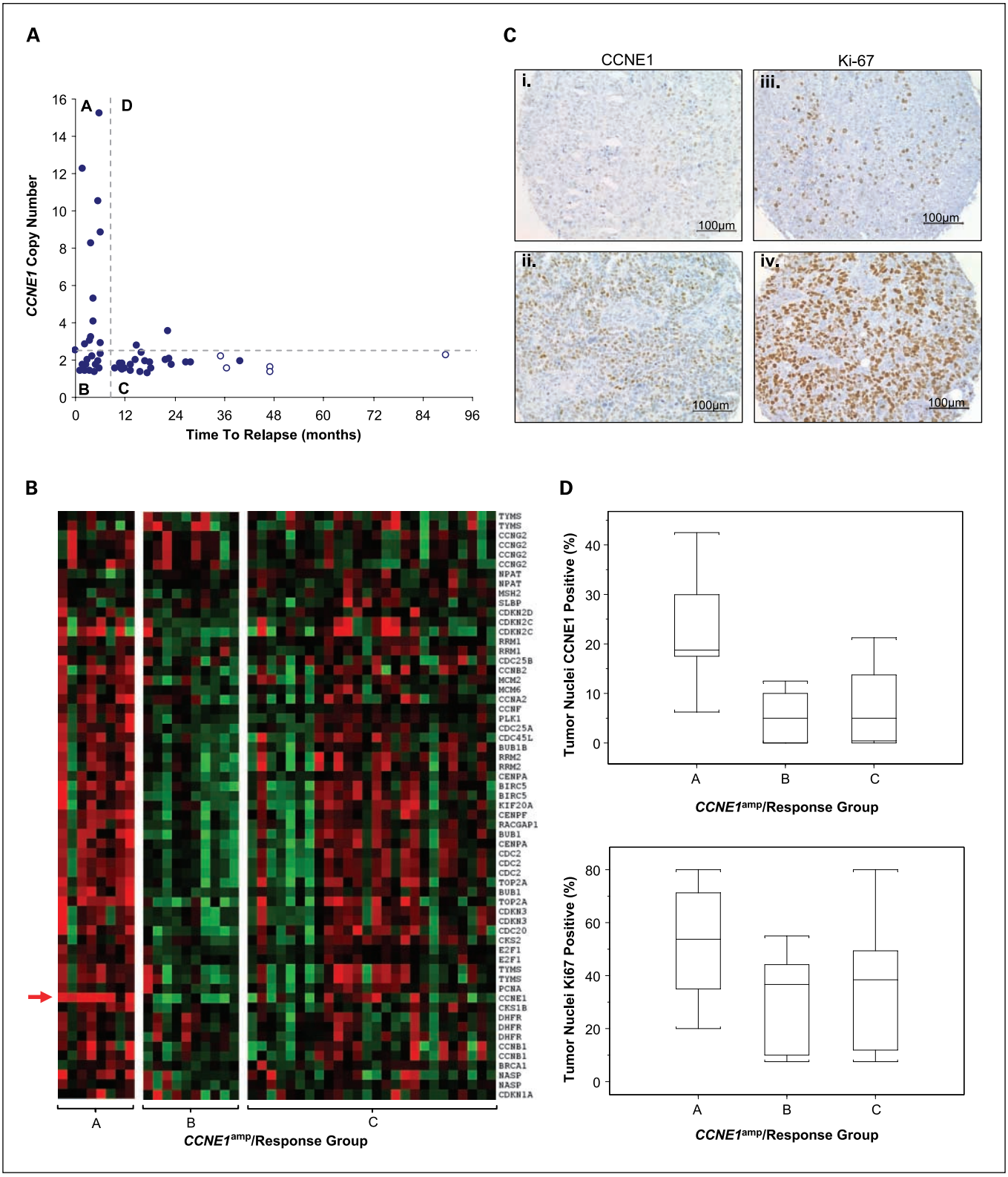

Fig. 3. Characterization of tumor subtypes classified by treatment response and *CCNE1* amplification status. *A,* samples stratified by treatment response (resistant, ‹6 mo PFS; responsive, ›9 mo PFS) and *CCNE1* amplification (*CCNE1*^{amp}) status as estimated by qPCR. Amplification is defined as a $\log_2$ copy number ratio ›0.3. Four subtypes are observed: group A (*CCNE1*-amplified, resistant), group B (*CCNE1*-unamplified, resistant), group C (*CCNE1*-unamplified, responsive), and group D (*CCNE1*-amplified, responsive). Clear circles, censored survival data. *B,* gene expression heat map of cell cycle genes in *CCNE1*^{amp}/response groups A, B, and C. Red, increased gene expression; green, decreased gene expression; arrow, *CCNE1* gene expression probe. *C,* example of tumor tissue with (*i*) 20% and (*ii*) 60% of cells with CCNE1 staining, and (*iii*) 10% and (iv) 90% of tumor cells with nuclear Ki-67 staining. *D*, box plots depict the range of immunohistochemical staining for *CCNE1*^{amp}/response groups A, B, and C for (*top*) CCNE1, P ‹ 0.02, and (*below*) Ki-67, P ‹ 0.28. Values for each sample taken as the average of up to four tissue microarray cores. A total of 5, 7, and 16 tumors from each group A, B, and C, respectively (n = 28) are represented.

Distinct gene expression changes in tumors from patients with or without* CCNE1 *amplification and poor treatment response. The association between *CCNE1* amplification and primary treatment resistance ranked as the most significant DMP associated with patient outcome and was consistent with previous studies (14). We therefore sought to better understand the molecular changes in tumors harboring amplification of the *CCNE1* locus and to contrast these with tumors from patients who had a poor response to treatment without *CCNE1* amplification.

A total of 47 samples, of the 85 samples analyzed using SNP microarrays, were also evaluated by qPCR and gene expression arrays. Samples were segregated into four groups (A to D) according to *CCNE1* amplification (as assessed by qPCR) and chemotherapy response status (Fig. 3A). The observed statistical significance of *CCNE1* amplification and poor treatment response was maintained in this sample subset ($P < 0.001$ by Fisher test; $P < 0.01$ association with PFS; Fig. 3A). Pair-wise comparisons of gene expression were then made between the resistant groups (A and B) and the *CCNE1*-unamplified responsive group (C) using a signal-to-noise metric for all genes. The top-ranking genes were then analyzed for overrepresentation of genes according to biological processes and molecular function categories using PANTHER (Protein ANalysis THrough Evolutionary Relationships) classification (Supplementary Table S9; ref. 32).

As expected, we found an enrichment of cell cycle–associated genes in samples with *CCNE1* amplification (group A; Fig. 3A) relative to cases with poor survival and no amplification of *CCNE1*. Figure 3B shows up-regulation of cell cycle–associated genes in the resistant samples with *CCNE1* amplification using a cell cycle gene set obtained from Whitfield et al. (33). Tumors from patients with a relatively good clinical outcome (group C; Fig. 3A) seemed to include a heterogeneous population of tumors with respect to up-regulation of cell cycle genes. In cases without *CCNE1* amplification but a short time to relapse, there was increased expression of genes with extracellular matrix structure, cell adhesion, and signaling molecular functions (group B; Fig. 3A; Supplementary Table S9).

Immunohistochemical staining of* CCNE1 *and Ki-67 are associated with specific tumor subtypes. Cyclin E and proliferation-related Ki-67 antigen immunohistochemical staining was done on tissue microarrays to provide protein level validation of *CCNE1* gene amplification and its association with cellular proliferation. Examples of tumor tissue with low- and high-level immunohistochemistry staining are shown in Fig. 3, including *CCNE1* amplification/chemoresponse groups A, B, and C. A significant difference among subtypes (A, B, and C) and degree of CCNE1 positively stained tumor nuclei ($P < 0.02$, Kruskal-Wallis rank sum test) was observed, with increased staining in tumors with *CCNE1* gene amplification.

The degree of Ki-67 staining was similar between treatment-resistant (groups A and B combined) and treatment-responsive (group C) groups when directly compared (median staining of ~40% in each class), suggesting no obvious association between cellular proliferation and chemoresponse. When samples were segregated further by *CCNE1* amplification status, a trend similar to that observed by gene expression analysis of cell-cycle markers was seen. Figure 3D shows increased median staining of Ki-67 in the resistant samples with *CCNE1* amplification (~55%) compared with those without *CCNE1* gene amplification (~40%). Treatment-responsive tumors seem to represent a heterogeneous population of tumors with or without increased cellular proliferation, with median Ki-67 staining similar to that of group B (*CCNE1*-unamplified, chemoresistant) tumors (~40%).

Discussion

To the best of our knowledge, our cohort of 118 cases provides the largest single sample set of ovarian cancers examined by high-resolution genome-wide copy number analysis to date, using 3-fold or more samples than most previous studies. We applied GISTIC, a novel approach to defining peak regions of genomic change, which has been shown to identify known oncogene and tumor suppressor gene loci with superior accuracy than other microarray analytical methods (30). The data confirms copy number variation events previously identified in ovarian cancer, such as amplification regions containing *CCNE1* (34), *NOTCH3* (35), *RSF1* (16), *PRKCI* (15), *MDS1-EVI1* (12), and *MYC* (24), and deletions of *WWOX* (36) and *RB1* (37). Novel copy number aberrations identified included amplification of 1q23.3, containing *NUF2* and *PBX1*; 6p23-p22.3, including the oncogene *DEK*; and 15q26.2-q26.3, containing the potential therapeutic target *IGF1R*. Detailed analysis of this global survey of gains and loss in ovarian cancer will be described elsewhere.[11]

To identify regions of copy number variation associated with primary treatment response, we explicitly chose a large group of cases with clinically defined response to primary treatment that were matched for stage, histology, grade, treatment regimen, and debulk status. Prior to deriving associations with clinical outcome variables, we had the option of either using the entire dataset to first define peak regions of copy number variation, or to define minimal regions of copy number variation for each response group separately. Separate analysis of response groups seems superior and makes sense intuitively, as heterogeneity between groups may obscure findings if the data are treated as a single entity. For example, analysis of the separate response cohorts identified a discrete peak near *NCOA3* in the treatment-resistant group (Fig. 2D), which has tentatively been linked to poor outcome in ovarian cancer (38). This observation, however, was masked in the analysis of the entire 118 tumors, where the 20q peak was mapped to 20q13.31-q13.32, distal to *NCOA3* (Fig. 2B and Supplementary Table S4).

This study seems to be the most robust analysis of primary response in ovarian cancer to date, incorporating high-resolution genome-wide analysis, expression profiling, the use of significant numbers of cases, and explicit clinicopathologic criteria in a single combined approach. Although a number of previous studies of ovarian cancer have sought to relate copy number variation to clinical outcome, only two (5, 6) have involved similar numbers of serous cancers to this study and these utilized much lower resolution, metaphase comparative genomic hybridization analysis. Consistent with Staebler et al., we saw no evidence of a higher average number of chromosomal aberrations in resistant patients, with many regions such as 3q26 and 8q24 showing frequent but equivalent change in

[11] Manuscript in preparation.

the two groups. In fact, a greater number of significant copy number variation overall was detected in the responsive group compared with the resistant group (40 peaks and 31 peaks, respectively; Supplementary Tables S5 and S6). The difference is most likely related to the larger size of the responsive cohort, allowing for the detection of additional low-frequency events.

In addition to our genome-wide discovery approach, we did the first head-to-head analysis of candidate genes associated with copy number variation and outcome in ovarian cancer as independent validation of previous findings. *CCNE1* was the only candidate taken from the literature where copy number was specifically associated with primary chemoresistance in our sample population. Discrepancy may relate to variation in methods used to detect copy number variation such as the sensitivity or resolution of microarray platforms (9, 12, 15, 17) or approaches taken in sample preparation. For example, laser-capture microdissection (9) or immunomagnetic separation (16) may have improved the ability to detect copy number variation in some studies, whereas the use of only whole tumor material (15, 17) or a lower percentage tumor content cutoff for needle dissection (12) may have obscured molecular correlations with outcome. Some of the selected candidate genes had previously been shown to correlate with PFS and/or OS, rather than categorical response to primary treatment *per se* and therefore may not have been validated in this cohort. For example, *ZNF217*, previously associated with OS (23), was associated with both PFS and OS in our analysis but not platinum resistance specifically. Furthermore, studies often varied in response definitions and survival end points used to derive clinical associations. For example, whereas some investigators have used progression-free interval, others have used pathologic/clinical response after treatment to derive response status (19, 21).

In this study, resistant cases had either progressive or stable disease during treatment or had a partial or complete CA125 response and relapsed within 6 months from the end of primary chemotherapy. When examined separately, there seemed to be no obvious distinction between these two modes of resistance and the presence of molecular prognostic markers (specifically, cyclin E amplification). However, as the number of samples from each category of resistance was low, a thorough statistical analysis could not be done.

SNP-based and qPCR copy number data were general highly concordant, although some differences were apparent that were primarily explained by poor representation of SNP markers in some regions (particularly for *MUC1* and *RAB25*), preventing accurate quantification of specific genes using flanking SNP markers. In addition, consistent with previous reports (39), we found that the amplification amplitude was lower with SNP data (Supplementary Fig. S2). Saturation of the SNP array probes at high copy number and/or smoothing of SNP data resulting in compression of copy number values likely accounts for quantitative differences between the observed qPCR and SNP data. Related to this, it is notable that we did not observe a statistically significant value for PFS using SNP data as a continuous variable for *CCNE1* (Table 3) although the association was clear using qPCR data. Specifically, all samples with high-level amplification of the *CCNE1* gene as assessed by qPCR ($\log_2$ ratio ≥ 2) were chemoresistant (Fig. 3A). The difference may be explained by SNP copy number underestimation of high-level gains (Supplementary Fig. S2).

Expression profiling was used to identify likely gene targets in each DMP and to validate associations with PFS and OS in samples additional to those analyzed by SNP microarray. The magnitude of fold change between chemoresponse groups was, in most cases, moderate (<1.5; Supplementary Table S7). This is probably due in part to the fact that mean gene expression differences between groups does not sufficiently account for molecular heterogeneity within groups, particularly where copy number variation occurs at low frequencies. We did, however, find analysis of gene expression associations with PFS and OS useful for narrowing down likely candidates for further validation studies.

Analysis of the SNP copy number data revealed amplifications associated with chemoresistance, involving two loci, each with highly relevant biological candidates within or near the mapped peak regions: *CCNE1* and *NCOA3*. Previous overexpression of the steroid receptor coactivator *NCOA3* (*AIB1*) in breast tumors, believed to interact with nuclear hormone receptors to enhance their transcriptional activity, has been shown to be significantly correlated with shorter PFS and OS (40). In ovarian tumors, although a trend towards amplification and poor OS has been observed, statistical significance was not shown (38). Interestingly, another potential target of 20q amplification including in our candidate gene screen, *ZNF217*, is located ~1.2 Mb away from the chromosome 20 DMP containing *NCOA3*. The *ZNF217* locus was not identified as a peak copy number variation significantly associated with platinum resistance in our cohort; in addition, it showed a lower statistical association with PFS and OS than *NCOA3*. Although it has been suggested that 20q involves a number of distinct amplicons (38), our findings suggest that *NCOA3* rather than *ZNF217* is the more likely target of 20q amplification events associated with resistance, with increased gene expression also significantly correlated with shorter PFS and OS (Supplementary Table S7). Given the size of the mapped DMP amplicon on 20q (>10 Mb), however, it is possible that additional gene(s) within the mapped region are important in tumorigenesis and treatment response. Identification of other drivers requires further systematic functional characterization of all genes within this region.

CCNE1 functions as a regulatory subunit of CDK2 essential for G_1 to S-phase transition and DNA replication, in addition to playing a role in apoptosis and chromosomal instability in tumor cells (41). CyclinE-cdk2 act through phosphorylation of substrates involved in G_1 progression, S-phase entry, and centrosome duplication, in addition to having kinase-independent functions involving loading mini-chromosome maintenance proteins onto replication origins, as quiescent cells enter the cell cycle (42).

CCNE1 gene amplification has been identified as a mechanism of overexpression in ovarian tumors with a direct correlation with poor outcome in this and previous studies (13, 14), although it had not been explicitly associated with primary treatment resistance until now. Previous studies associating *CCNE1* with poor outcome in ovarian cancer involved samples drawn from the US Gynecological Oncology Group bank (14) and from German patients (13). Our study included patients from Australia, Norway, and Japan. Collectively, these findings indicate that *CCNE1* amplification is likely to be a marker of primary treatment failure and poor outcome in patients from diverse ethnic backgrounds.

Although the independent identification of the *CCNE1* amplicon in these studies suggests that is the dominant region of copy number gain associated with poor outcome in ovarian cancer, the mechanism of resistance is unclear. We find that *CCNE1* amplification led to expression of cell cycle–associated genes. Accelerated repopulation of tumor cells after treatment is a potential mechanism of treatment failure (43) that may be facilitated by *CCNE1* amplification in cells "hard-wired" for increased proliferative capacity. However, we also see increased expression of cell cycle genes in the treatment-responsive primary tumors. In addition, increased proliferation, including via forced expression of *CCNE1* in ovarian cells *in vitro* (44), has previously been linked to chemosensitivity rather than chemoresistance (45, 46). Taken together, these seemingly contradictory findings suggest that cellular proliferation alone may not account for response to chemotherapy. Recently, *CCNE1* has been reported to have a role in mediating asymmetric cell division, specifying cell fate and, importantly, in driving stem cell self-renewal, independent of its activity in cellular proliferation (47, 48). Enhanced self-renewal may provide a novel mechanism for treatment failure in patients with tumors bearing a *CCNE1* amplification.

Although there was no statistically significant difference in grade between resistant and responsive groups, we note that four cases of grade 1 serous carcinoma were included in the responsive group (Table 1). Interestingly, one low-grade sample represented in the resistant group contained a *CCNE1* amplification and is represented in group A (Fig. 3), suggesting that *CCNE1* amplification and poor outcome are not exclusive to high-grade tumors.

By applying gene expression analysis to samples from resistant patients without *CCNE1* amplification, we were able define a distinct molecular subtype of resistant cases characterized by increased extracellular matrix–associated markers. This finding is consistent with our recent analysis of serous tumors that identified a molecular subtype characterized by extracellular matrix, matrix remodeling, and stromal response that was strongly associated with desmoplastic response and poor survival (25). A florid stromal reaction may reflect a host response aimed at containing an aggressive tumor or, alternatively, may directly participate in driving tumor growth (49). Recent findings also indicate that collagen deposition and tumor microenvironment may play a direct role in chemoresistance (50).

In conclusion, we have highlighted biologically aggressive tumors with *CCNE1* or *NCOA3* amplifications and the role of extracellular matrix in strongly influencing clinical chemoresistance. Given that *CCNE1* amplification seems to be consistently associated with short response time (our study) and poor survival (our findings and others), priority should be placed on determining the appropriateness of directing patients carrying *CCNE1* amplification for trials with novel treatments, either directly targeting *CCNE1* or downstream pathway members. Furthermore, non–tumor-centric modes of resistance associated with host tissue elements, such as the extracellular matrix or activated stroma, may require alternative therapeutic strategies.

Disclosure of Potential Conflicts of Interest

No potential conflicts of interest were disclosed.

Acknowledgments

We thank Britt Edvardsen, Melanie Trivett, and Elena Takano for their technical assistance, in addition to Maurice Loughrey for additional pathologic review of tissue samples.

We gratefully acknowledge the cooperation of the following institutions associated with the Australian Ovarian Cancer Study: New South Wales: John Hunter Hospital, North Shore Private Hospital, Royal Hospital for Women, Royal North Shore Hospital, Royal Prince Alfred Hospital, Westmead Hospital; Queensland: Mater Misericordiae Hospital, Royal Brisbane and Women's Hospital, Townsville Hospital, Wesley Hospital; South Australia: Flinders Medical Centre, Queen Elizabeth II, Royal Adelaide Hospital; Tasmania: Royal Hobart Hospital; Victoria: Freemasons Hospital, Mercy Hospital for Women, Monash Medical Centre, Royal Women's Hospital; Western Australia: King Edward Memorial Hospital, St John of God Hospitals Subiaco, Sir Charles Gairdner Hospital, Western Australia Research Tissue Network (WARTN): and the Westmead Gynaecological Oncology Tissue Bank, a member of the Australasian Biospecimens Network-Oncology group.

We also acknowledge the contribution of the AOCS Management Group: D. Bowtell, G. Chenevix-Trench, A. Green, P. Webb, A. deFazio, D. Gertig, the study nurses and research assistants, and express our gratitude to all women who participated in the study.

References

1. Harries M, Gore M. Part I: chemotherapy for epithelial ovarian cancer -treatment at first diagnosis. Lancet Oncol 2002;3:529–36.
2. Bookman MA. Standard treatment in advanced ovarian cancer in 2005: the state of the art. Int J Gynecol Cancer 2005;15 Suppl 3:212–20.
3. Kelland L. The resurgence of platinum-based cancer chemotherapy. Nat Rev Cancer 2007;7:573–84.
4. Pinkel D, Albertson DG. Comparative genomic hybridization. Annu Rev Genomics Hum Genet 2005;6:331–54.
5. Partheen K, Levan K, Osterberg L, Helou K, Horvath G. Analysis of cytogenetic alterations in stage III serous ovarian adenocarcinoma reveals a heterogeneous group regarding survival, surgical outcome, and substage. Genes Chromosomes Cancer 2004;40:342–8.
6. Staebler A, Karberg B, Behm J, et al. Chromosomal losses of regions on 5q and lack of high-level amplifications at 8q24 are associated with favorable prognosis for ovarian serous carcinoma. Genes Chromosomes Cancer 2006;45:905–17.
7. Kim SW, Kim JW, Kim YT, et al. Analysis of chromosomal changes in serous ovarian carcinoma using high-resolution array comparative genomic hybridization: potential predictive markers of chemoresistant disease. Genes Chromosomes Cancer 2007;46:1–9.
8. Bernardini M, Lee CH, Beheshti B, et al. High-resolution mapping of genomic imbalance and identification of gene expression profiles associated with differential chemotherapy response in serous epithelial ovarian cancer. Neoplasia 2005;7:603–13.
9. Birrer MJ, Johnson ME, Hao K, et al. Whole genome oligonucleotide-based array comparative genomic hybridization analysis identified fibroblast growth factor 1 as a prognostic marker for advanced-stage serous ovarian adenocarcinomas. J Clin Oncol 2007;25:2281–7.
10. Osterberg L, Levan K, Partheen K, Helou K, Horvath G. Cytogenetic analysis of carboplatin resistance in early-stage epithelial ovarian carcinoma. Cancer Genet Cytogenet 2005;163:144–50.
11. Suzuki S, Moore DH, Ginzinger DG, et al. An approach to analysis of large-scale correlations between genome changes and clinical endpoints in ovarian cancer. Cancer Res 2000;60:5382–5.
12. Nanjundan M, Nakayama Y, Cheng KW, et al. Amplification of MDS1/EVI1 and EVI1, located in the 3q26.2 amplicon, is associated with favorable patient prognosis in ovarian cancer. Cancer Res 2007;67:3074–84.
13. Mayr D, Kanitz V, Anderegg B, et al. Analysis of gene amplification and prognostic markers in ovarian cancer using comparative genomic hybridization for microarrays and immunohistochemical analysis for tissue microarrays. Am J Clin Pathol 2006;126:101–9.
14. Farley J, Smith LM, Darcy KM, et al. Cyclin E expression is a significant predictor of survival in advanced, suboptimally debulked ovarian epithelial cancers: a Gynecologic Oncology Group study. Cancer Res 2003;63:1235–41.
15. Eder AM, Sui X, Rosen DG, et al. Atypical PKCiota contributes to poor prognosis through loss of apical-basal polarity and Cyclin E overexpression in ovarian cancer. Proc Natl Acad Sci U S A 2005;102:12519–24.
16. Shih Ie M, Sheu JJ, Santillan A, et al. Amplification of a chromatin remodeling gene, Rsf-1/HBXAP, in ovarian carcinoma. Proc Natl Acad Sci U S A 2005;102:14004–9.
17. Cheng KW, Lahad JP, Kuo WL, et al. The RAB25 small GTPase determines aggressiveness of ovarian

and breast cancers. Nat Med 2004;10:1251–6. Epub 2004 Oct 24.

18. Kato H, Arakawa A, Suzumori K, Kataoka N, Young SR. FISH analysis of BRCA1 copy number in paraffin-embedded ovarian cancer tissue samples. Exp Mol Pathol 2004;76:138–42.

19. Lassus H, Leminen A, Vayrynen A, et al. ERBB2 amplification is superior to protein expression status in predicting patient outcome in serous ovarian carcinoma. Gynecol Oncol 2004;92:31–9.

20. Slamon DJ, Godolphin W, Jones LA, et al. Studies of the HER-2/neu proto-oncogene in human breast and ovarian cancer. Science 1989;244:707–12.

21. Takano M, Fujii K, Kita T, Kikuchi Y, Uchida K. Amplicon profiling reveals cytoplasmic overexpression of MUC1 protein as an indicator of resistance to platinum-based chemotherapy in patients with ovarian cancer. Oncol Rep 2004;12:1177–82.

22. Makhija S, Sit A, Edwards R, et al. Identification of genetic alterations related to chemoresistance in epithelial ovarian cancer. Gynecol Oncol 2003;90:3–9.

23. Peiro G, Diebold J, Lohrs U. CAS (cellular apoptosis susceptibility) gene expression in ovarian carcinoma: correlation with 20q13.2 copy number and cyclin D1, p53, and Rb protein expression. Am J Clin Pathol 2002;118:922–9.

24. Baker VV, Borst MP, Dixon D, Hatch KD, Shingleton HM, Miller D. c-myc amplification in ovarian cancer. Gynecol Oncol 1990;38:340–2.

25. Tothill RW, Tinker AV, George J, et al. Novel molecular subtypes of serous and endometrioid ovarian cancer linked to clinical outcome. Clin Cancer Res. In press.

26. Chi DS, Eisenhauer EL, Lang J, et al. What is the optimal goal of primary cytoreductive surgery for bulky stage IIIC epithelial ovarian carcinoma (EOC)? Gynecol Oncol 2006;103:559–64.

27. Rustin GJ, Nelstrop AE, Tuxen MK, Lambert HE. Defining progression of ovarian carcinoma during follow-up according to CA 125: a North Thames Ovary Group Study. Ann Oncol 1996;7:361–4.

28. Vergote I, Rustin GJ, Eisenhauer EA, et al. Re: new guidelines to evaluate the response to treatment in solid tumors [ovarian cancer]. Gynecologic Cancer Intergroup. J Natl Cancer Inst 2000;92:1534–5.

29. Matsuzaki H, Dong S, Loi H, et al. Genotyping over 100,000 SNPs on a pair of oligonucleotide arrays. Nat Methods 2004;1:109–11.

30. Beroukhim R, Getz G, Nghiemphu L, et al. Assessing the significance of chromosomal aberrations in cancer: methodology and application to glioma. Proc Natl Acad Sci U S A 2007;104:20007–12.

31. Rozen S, Skaletsky H. Primer3 on the WWW for general users and for biologist programmers. Methods Mol Biol 2000;132:365–86.

32. Mi H, Guo N, Kejariwal A, Thomas PD. PANTHER version 6: protein sequence and function evolution data with expanded representation of biological pathways. Nucleic Acids Res 2007;35:D247–52.

33. Whitfield ML, George LK, Grant GD, Perou CM. Common markers of proliferation. Nat Rev Cancer 2006;6:99–106.

34. Snijders AM, Nowee ME, Fridlyand J, et al. Genome-wide-array-based comparative genomic hybridization reveals genetic homogeneity and frequent copy number increases encompassing CCNE1 in fallopian tube carcinoma. Oncogene 2003;22:4281–6.

35. Park JT, Li M, Nakayama K, et al. Notch3 gene amplification in ovarian cancer. Cancer Res 2006;66:6312–8.

36. Paige AJ, Taylor KJ, Taylor C, et al. WWOX: a candidate tumor suppressor gene involved in multiple tumor types. Proc Natl Acad Sci U S A 2001;98:11417–22.

37. Gorringe KL, Jacobs S, Thompson ER, et al. High-resolution single nucleotide polymorphism array analysis of epithelial ovarian cancer reveals numerous microdeletions and amplifications. Clin Cancer Res 2007;13:4731–9.

38. Tanner MM, Grenman S, Koul A, et al. Frequent amplification of chromosomal region 20q12–13 in ovarian cancer. Clin Cancer Res 2000;6:1833–9.

39. Zhao X, Li C, Paez JG, et al. An integrated view of copy number and allelic alterations in the cancer genome using single nucleotide polymorphism arrays. Cancer Res 2004;64:3060–71.

40. Zhao C, Yasui K, Lee CJ, et al. Elevated expression levels of NCOA3, TOP1, and TFAP2C in breast tumors as predictors of poor prognosis. Cancer 2003;98:18–23.

41. Hwang HC, Clurman BE. Cyclin E in normal and neoplastic cell cycles. Oncogene 2005;24:2776–86.

42. Geng Y, Lee YM, Welcker M, et al. Kinase-independent function of cyclin E. Mol Cell 2007;25:127–39.

43. Kim JJ, Tannock IF. Repopulation of cancer cells during therapy: an important cause of treatment failure. Nat Rev Cancer 2005;5:516–25.

44. Bedrosian I, Lu KH, Verschraegen C, Keyomarsi K. Cyclin E deregulation alters the biologic properties of ovarian cancer cells. Oncogene 2004;23:2648–57.

45. Kolfschoten GM, Hulscher TM, Pinedo HM, Boven E. Drug resistance features and S-phase fraction as possible determinants for drug response in a panel of human ovarian cancer xenografts. Br J Cancer 2000;83:921–7.

46. Jazaeri AA, Awtrey CS, Chandramouli GV, et al. Gene expression profiles associated with response to chemotherapy in epithelial ovarian cancers. Clin Cancer Res 2005;11:6300–10.

47. Chia W, Prokopenko SN. Cyclin E at the centre of an identity crisis. Nat Cell Biol 2005;7:3–5.

48. Chia W, Somers WG, Wang H. Drosophila neuroblast asymmetric divisions: cell cycle regulators, asymmetric protein localization, and tumorigenesis. J Cell Biol 2008;180:267–72.

49. Olumi AF, Grossfeld GD, Hayward SW, Carroll PR, Tlsty TD, Cunha GR. Carcinoma-associated fibroblasts direct tumor progression of initiated human prostatic epithelium. Cancer Res 1999;59:5002–11.

50. Sherman-Baust CA, Weeraratna AT, Rangel LB, et al. Remodeling of the extracellular matrix through overexpression of collagen VI contributes to cisplatin resistance in ovarian cancer cells. Cancer Cell 2003;3:377–86.